



This is a repository copy of *A fragmentation assessment method for submerged charges*.

White Rose Research Online URL for this paper:

<https://eprints.whiterose.ac.uk/220930/>

Version: Accepted Version

Proceedings Paper:

Nowak, P., Waddoups, R., Farrimond, D. orcid.org/0000-0002-9440-4369 et al. (7 more authors) (2024) A fragmentation assessment method for submerged charges. In: Proceedings of The 19th International Symposium on Interaction of the Effects of Munitions with Structures (ISIEMS). 19th International Symposium on Interaction of the Effects of Munitions with Structures (ISIEMS), 09-13 Dec 2024, Bonn, Germany. International Symposium on Interaction of the Effects of Munitions with Structures (ISIEMS)

© 2024 ISIEMS. This is an author-produced version of a paper subsequently published in Proceedings of The 19th International Symposium on Interaction of the Effects of Munitions with Structures (ISIEMS). Uploaded with permission from the copyright holder.

Reuse

Items deposited in White Rose Research Online are protected by copyright, with all rights reserved unless indicated otherwise. They may be downloaded and/or printed for private study, or other acts as permitted by national copyright laws. The publisher or other rights holders may allow further reproduction and re-use of the full text version. This is indicated by the licence information on the White Rose Research Online record for the item.

Takedown

If you consider content in White Rose Research Online to be in breach of UK law, please notify us by emailing eprints@whiterose.ac.uk including the URL of the record and the reason for the withdrawal request.



eprints@whiterose.ac.uk
<https://eprints.whiterose.ac.uk/>

Distribution: For public release

A fragmentation assessment method for submerged charges.

Piotr Nowak¹, Ross Waddoups^{2,4}, Dain Farrimond^{2,4}, Tomasz Gajewski¹, Tommy Lodge^{2,4}, Genevieve Langdon², Andy Tyas^{2,4}, Piotr Sielicki¹, Elliot Tam³, Mark Whittaker³

piotr.nowak@doctorate.put.poznan.pl – Poznan University of Technology, pl. M. Skłodowskiej-Curie 5, 60-965 Poznan, Poland

1 Poznan University of Technology, Poland

2 University of Sheffield, United Kingdom

3 Defence Science and Technology Laboratory, United Kingdom

4 Blastech Ltd., United Kingdom

Keywords: ordnance disposal, underwater explosion, combined effects, blast, fragments

Abstract

Explosive ordnance poses a threat to human life, local ecosystems and infrastructure. During the detonation of cased munitions, the rapid energy release from the chemical process is transferred to the surrounding material, resulting in fragmentation. This can cause additional damage on top of the air blast. During land ordnance disposal, these two hazard mechanisms are considered to ensure safe working distances of operatives and infrastructure. However, underwater ordnance clearance often omits or ignores the risk of fragmentation. This method may be justified when clearing ordnance in deeper seas, as fragmentation can only propagate so far within water. Nevertheless, most explosive ordnance disposal operations take place in shallow waters, close to shorelines or near critical maritime infrastructure - meaning a likelihood of fragmentation damage. This paper presents a series of experimental trials that compare both air and underwater cased explosive charges at various depths to investigate the characteristics and distribution of the associated fragmentation. Both high-speed videography and witness panels were employed to capture in-flight velocities and fragment distribution to improve safe working procedures for naval ordnance operations.

Introduction

Munition disposal operations are considered unplanned and time-limited actions. The blast and fragmentation parameters on land for commonly used explosive weapons are well characterized in the manufacturer's documentation [1], military regulations and procedures [2], explosive safety standards [3], or scientific research [4].

Fragments are explosively driven projectiles resulting from the failure of casing materials, usually of irregular mass and shape [3]. The hazard level associated with fragmenting casings is governed by the probability of interaction and the kinetic energy of the projectile at the point of interaction [5].

National and international publications concerning fragmentation and blast hazards [2,3] recommend simple mathematical formulae and tables to estimate the physical effect of munition detonation in open-air scenarios. Despite general procedures for fragmentation prediction being available for a given net explosive quantity (NEQ), results suggest that when comparing the performance of similar-sized warheads, the fragmentation patterns also depend on the explosive composition and casing shape. For explosive projectiles, from 122 mm to 128 mm in diameter, Zecevic et al. [6] found that the vast majority of fragments cover the lateral and rear sides of the ordnance. The area located in the front of the projectiles was considered relatively safe as no, or minimum, lethal spray was observed during tests. An improved warhead design and a more energetic material increased the munition lethal zone.

The danger area can be estimated based on the total mass of explosive (or its TNT equivalent) and subjective and objective safety criteria or factors. Any additional information on the type of ordnance, its condition, location and position to other objects and obstacles allows for a better assessment of the detonation effects, but are judged on a case-by-case basis.

Predicting fragment distribution of weapons is complex due to the variability in size, mass and shape of a given casing piece. There is, therefore, a need to compare ideal and real-world fragments from cased charges. Qi et al [7] investigated the flight characteristics and momentum transfer of a blast-driven bearing ball embedded in a cylindrical charge, both experimentally and numerically, when the explosive was detonated in air. The spherical steel orb, commonly used in improvised explosive devices (IED), represents an ideal fragment of known mass and shape. Even though the detonation causes a deformation of the sphere, the average mass loss does not exceed 3 %. The mass of a single orb can be used for further analysis e.g. predicting the kinetic energy on impact.

Water is often used as a deceleration medium in fragmentation studies [8]. In this way, the number of natural fragments and their mass can be obtained for further analysis without considering the fragment hazard. The properties of water can suppress the air blast of an explosion. For example, adding a water curtain in front of a perforated plate reduced the overpressure and impulse behind the barrier [9]. Water-filled bags presented by Salter [10] can dramatically reduce the blast, thermal radiation and the speed of fragments, helping to protect key infrastructure.

Some experimental studies have indicated that projectile fragments propelled into the air by underwater detonation may pose a lethal threat at long ranges, although limited data is available [11,12]. Swisdak and Montanaro [11] proposed a method for estimating the maximum fragment range corresponding to the scaled explosion depth. The prediction equation was developed based on shallow water tests of the MK 82 bomb, during which maximum range, fragment velocity, and fragment mass were recorded. The characteristics of underwater fragmentation were also described by Lee and Rude [12] for smaller charges of 143 g C4 placed at a 0.45 m depth. The dispersing process and damage potential of heavy steel casing with a charge/weight ratio of 7 % were examined. An underwater charge produces abnormally large fragments compared to an air detonation, carrying greater kinetic energy and therefore a greater danger.

This paper focuses on the fragmentation hazard related to underwater ordnance. Conducting full-scale trials is costly and high-risk so a laboratory-scale methodology has been implemented utilising small-scale charges. The use of reduced scale test facilities has previously been proven effective in free-air [13] blast parameter characterisation at the University of Sheffield.

In this paper, results from 30 explosive tests involving underwater detonations are reported with the aim of elucidating the influence of charge depth and casing type on the fragmentation risk. The charges were prepared with a constant charge mass, surrounded by three types of steel casings and placed at varying depths within the water medium. The fragmentation pattern, flight parameters and quantity of fragments for selected depth of burst are presented.

A real-life dilemma

The naval mine illustration (Figure 1) shows the problem of removing a sunken weapon with a high explosive content. For land UXO disposal, a straightforward procedure needs to be followed to ensure public safety. Blast and fragmentation safe distances have to be calculated or obtained from tables, charts and risk assessment tools [2,14]. To dispose of ordnance found in shallow waters near ports, shores and harbours is a more complex task [15,16]. The choice of the disposal method is preceded by a detailed analysis. An underwater shock wave can damage critical underwater infrastructure, deadly pressure values for humans and animals are transmitted long distances from the source, and countermeasures are extremely expensive and therefore time-consuming [17]. In the author's opinion, the properties of water are favourable for specialised clearance groups, because even a few meters of water suppress thermal radiation, shock waves and fragmentation.

In 2020, a naval mine filled with 800 kg of high explosive (HE) was discovered in Poland next to an inland waterway at the depth of 10 m and posed a real threat to marine traffic. In favourable conditions, such objects can be lifted and transported (towed) to a disposal area. Such a procedure carries a high risk, adds a fragmentation hazard and extends the duration of the operation, which should be taken into account when planning tasks in a civilian environment. It is often difficult to assess the effect of depth on the number of fragments and maximum throw distance in real-life situations, but by lifting the weapon to the surface we risk exposing military personnel to shrapnel.

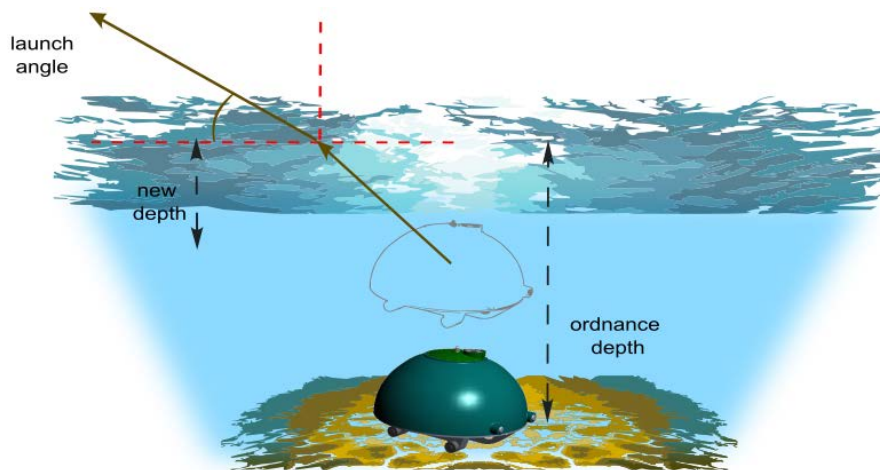


Figure 1. Illustrative drawing of the naval mine.

For those reasons during disposal operations, an underwater mine or bomb is transported in the water, with the maximum fragmentation distance on land used as the evacuation distance. This approach leads to an overestimation in the hazard zone size. General procedures advise a minimum towing distance, however the depth of towing is not considered as important.

Test Methods for Fragmentation Assessment

The 30 small-scale experimental tests were carried out in a steel water tank at the University of Sheffield Blast and Impact laboratory. A simplified end-detonated cylindrical cased charge of 46.5 ± 0.5 g PE10 explosive was used for all tests. Before each test, the charge was suspended inside the tank and 20 new strawboard witness panels (1500x750x3.7 mm, long centreline parallel to the cylinder axis) were placed above the explosives to capture flying shrapnel. A constant distance of 600 mm from the panels to the centre of the charge was maintained throughout the experiment (Figure 2). The water was filled to a pre-determined height to assess the influence of charge placement within shallow water scenarios on fragmentation behaviour.

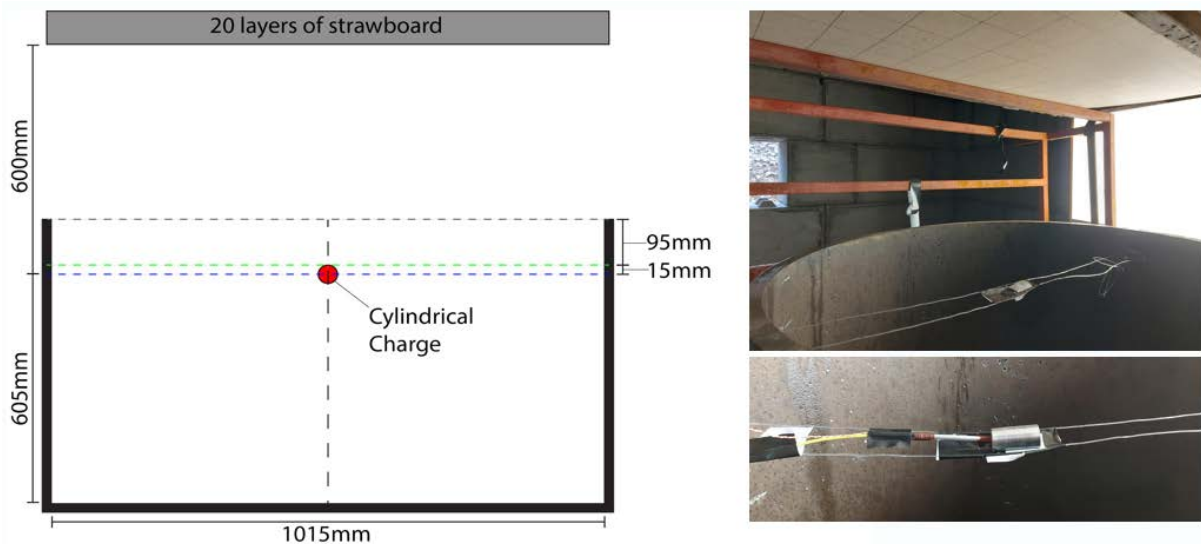


Figure 2. Illustrative drawing of the experimental setup and charge placement in the tank.

Three types of steel casing were used to evaluate the fragmentation phenomena. The primary case design was a steel machined liner intended to replicate a typical munition body. The number and size of natural fragments vary from test to test due to the random division of the casing material. To obtain the behaviour of idealised fragmentation, two sizes of spherical steel orbs were selected and enclosed in a 3D-printed jacket (Figure 3). The diameter of the small steel ball was selected at 1.7 mm to allow for a total mass which reflects the mass of the steel liner of avg. 37 g. The third fragmentation material was the 2.6 mm diameter orb with a total steel shell mass of 61 g. By arranging the orbs in a 3D-printed housing, an average of 1,860 fragments were obtained for small orbs and 875 for larger ones. The selected charge/total mass ratio of 43 % and 55 % matches the value of popular large-size weapons, such as aerial bombs and naval mines often found near coastal cities [17].

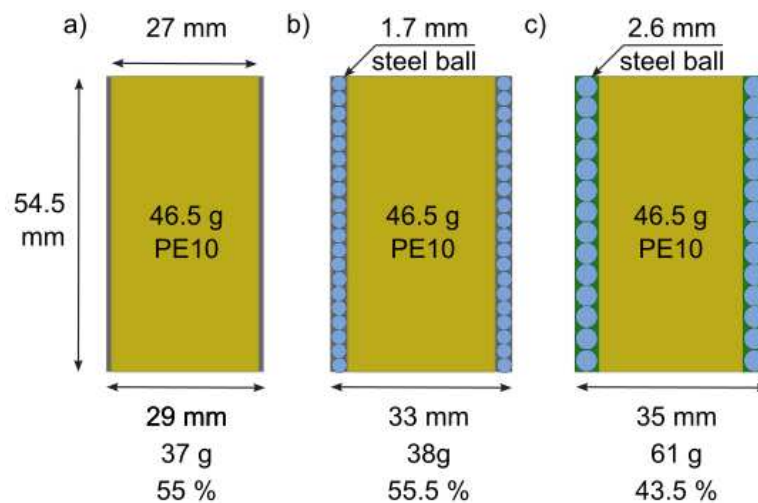


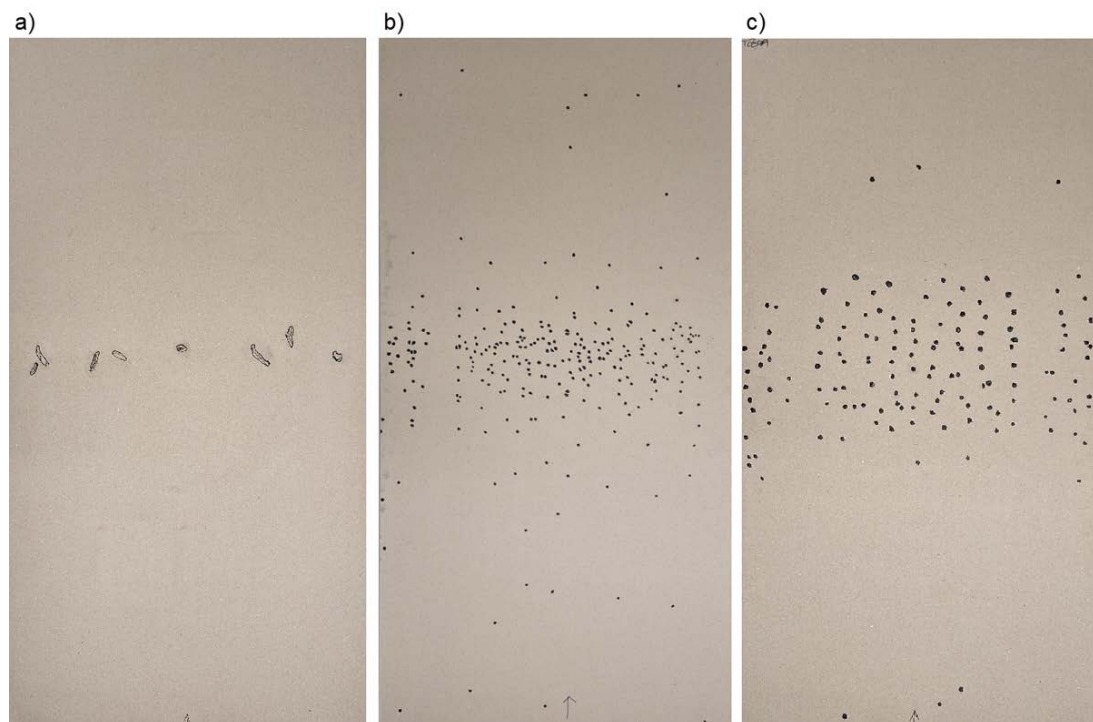
Figure 3. Cased charge design: (a) machined liner, (b) 1.7 mm steel ball, (c) 2.6 mm steel ball.

To obtain reference data, four air shots (setup A) were prepared: two with machined liner and two with 1.7 mm ball casing. The remaining 26 tests with selected water levels in the tank were designed to assess the impact of the depth of burst on the fragment's parameters. Those tests were divided into series depending on the relative location of the casing to the surface: half-submerged, charge top at the surface, 45 mm and 95 mm depth (test setup B, C, D, E), all of which are detailed in Table 1.

Table 1. Shots summary.

	Type of shell	Test setup	Pierced layers	Number of repetition	Fragments number	Percentage of steel mass (%)
1	Liner	(A) air	13	2	190	11.3
2	1.7 mm ball	(A) air	9	2	285	15.3
3	Liner	(B) half-submerged	14	3	165	11.9
4	1.7 mm ball	(B) half-submerged	9	2	322	17.2
5	2.6 mm ball	(B) half-submerged	10	1	233	26.7
6	Liner	(C) charge top at surface	13	3	124	13.1
7	1.7 mm ball	(C) charge top at surface	6	3	306	16.4
8	Liner	(D) 45 mm depth	4	2	11	16.9
9	1.7 mm ball	(D) 45 mm depth	4	2	319	17.1
10	2.6 mm ball	(D) 45 mm depth	3	2	164	18.7
12	Liner	(E) 95 mm depth	0	3	1	1.2
13	1.7 mm ball	(E) 95 mm depth	1	2	2	0.3
14	2.6 mm ball	(E) 95 mm depth	1	2	116	13.3

A fixed charge was centrally detonated using a non-electrical detonator (0.8 g TNT equivalent mass of explosive). All witness panels were carefully inspected for holes and embedded fragments, and then highlighted with a black marker for better contrast. The penetration pattern of each strawboard panel was photographed (Figure 4) and converted into numerical data. The number of penetrated cards was recorded. A high-speed camera was used to record the fragmentation process in low light conditions at a rate of 100,000 - 150,000 frames/sec.

**Figure 4** Fragmentation pattern for a) machined liner, b) 1.7 mm, c) 2.6 mm steel balls.

Interpretation of witness panel results

The results of the fragmentation witness panel capture analysis and the percentage of the original casing mass was recorded in Table 1. There are clear trends that represent the influence of water on the number of fragments which were able to interact with the panels. The total steel mass recovered is a good indicator of the quantity of casing material but provides limited indication of the directionality for hazard scenarios. Clearly, at depths of 95 mm, the fragmentation hazard above the water surface is reduced. However, for all other charge locations, it is difficult to determine safety regions related to fragmentation parameters. To assess this, fragmentation tracking methods using high-speed imaging processing techniques have been developed.

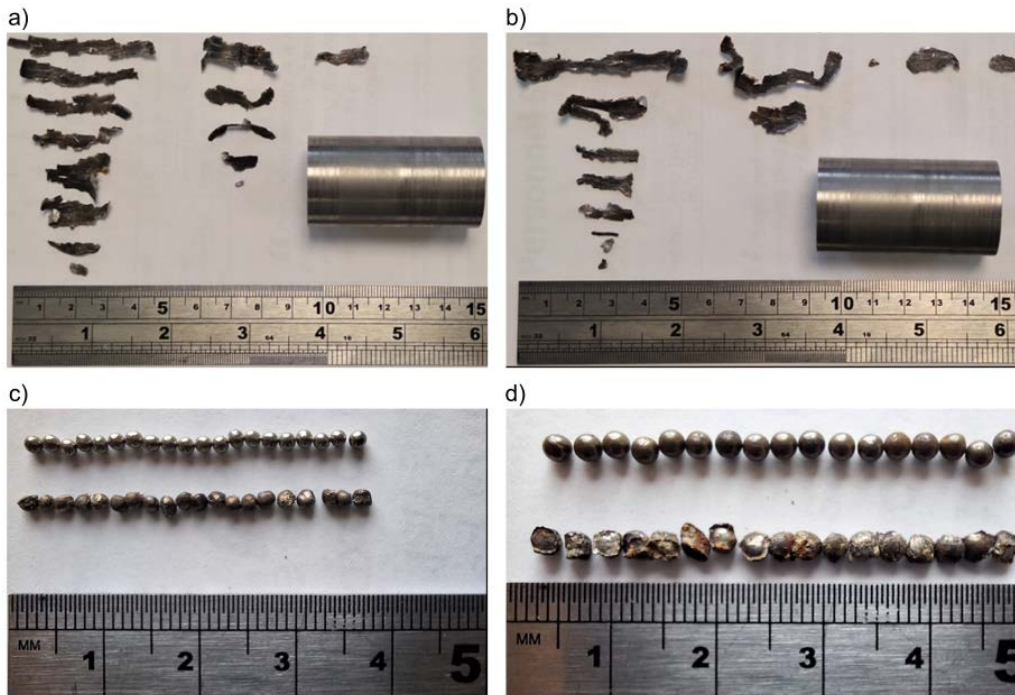


Figure 5. Machined liner (a), (b), 1.7 mm steel balls (c) and 2.6 mm steel balls (d) appearance after detonation.

During nominally identical trials, the steel liner casing produced a variable number of fragments of random mass and shape. The size of the collected pieces in the dry shots (setup A) was much smaller than for the wet tests, reaching only 25 mm length, but with largest number of impact traces and most of them weighing less than 0.01 g. Fully submerged charges produced a smaller number of fragments, but of greater individual size, up to 55 mm long. The maximum mass of a single shrapnel was 1.7 g (setup D, 45 mm depth), which constituted 4% of the total mass of the casing. This fragment penetrated only two layers of the strawboard panels, hitting the target flat (with the largest cross-sectional area). The highest value of kinetic energy does not necessarily translate into the penetration depth because it depends on the shape and impact angle at the target.

A comparison of two tests at a depth of 45 mm, Figure 5 (a) and (b), shows the randomness of the fragmentation process. The average recovered steel mass that hit the target was higher in these tests, 6.3 g (16.9 % of the liner mass), compared to 4.2 g (11.3 %) for the air test. The average mass of fragments in the half-submerged test was equal to 4.4 g (11.9%) and the subsurface charge of 4.8 g (13.1%) was also greater than in the air test (without water interaction). The total mass of fragments increased with increasing depth of burst (up to 45 mm) and drastically decreased to an average of 0.45 g (1.2 %) for a depth of 95 mm. These results may be due to the ratio of very small to large fragments as well as the expansion of the gas bubble pushing the water upwards and with it the smallest shell particles.

At greater depths, the main impact on fragments is likely water resistance, and the effect of the gas sphere is weaker. A similar phenomenon occurred in the case of 1.7 mm diameter balls. After the reference air detonation, 5.8 g (15.3%) of the steel casing mass was trapped in the strawboard plates.

Again, the total mass of fragments was rising in setup B (6.2 g, 16.4%), C (6.6 g, 17.2%) and D (6.5 g, 17.1%) to drop to 0.1 g (0.3%) at 95 mm depth in setup E. There was no reference air test for 2.6 mm diameter balls, but the number of fragment traces on the first panel decreased with depth. The corresponding fragment mass was 16.3 g (26.7%) for setup B, 11.4 g (18.7%) for setup D and 8.1 g (13.3%) for setup E.

In case of steel ball bearings, the number of impacts in the first witness panel can be directly related to the total mass of the fragments that impacting the target. Each ball had the same mass (0.0204 g for the 1.7 mm or 0.0698 g for 2.6 mm diameter balls). In both cases, shown in Figure 5 (c) and (d), a slight deformation and flattening of the balls on the side nearest the explosive was observed, with an average mass loss not exceeding 2% to 3%. The kinetic energy and penetration depth depend mainly on the impact velocity.

Figure 6 shows the fragment density on the strawboard panels for a liner shell detonation in two test setups: in the air and charge top at surface. A significant reduction in the number of fragments (from 190 to 124) was observed due to interaction with water. If we consider the initiation side as the tail and the opposite side as the nose of the payload, we can compare the distribution of fragments on the witness panels in a Cartesian coordinate system, and a polar coordinate system depending on the distance from the centre and angle from nose. Red lines and circles represent the impact traces on the right side and the blue on the left side of the strawboard panel.

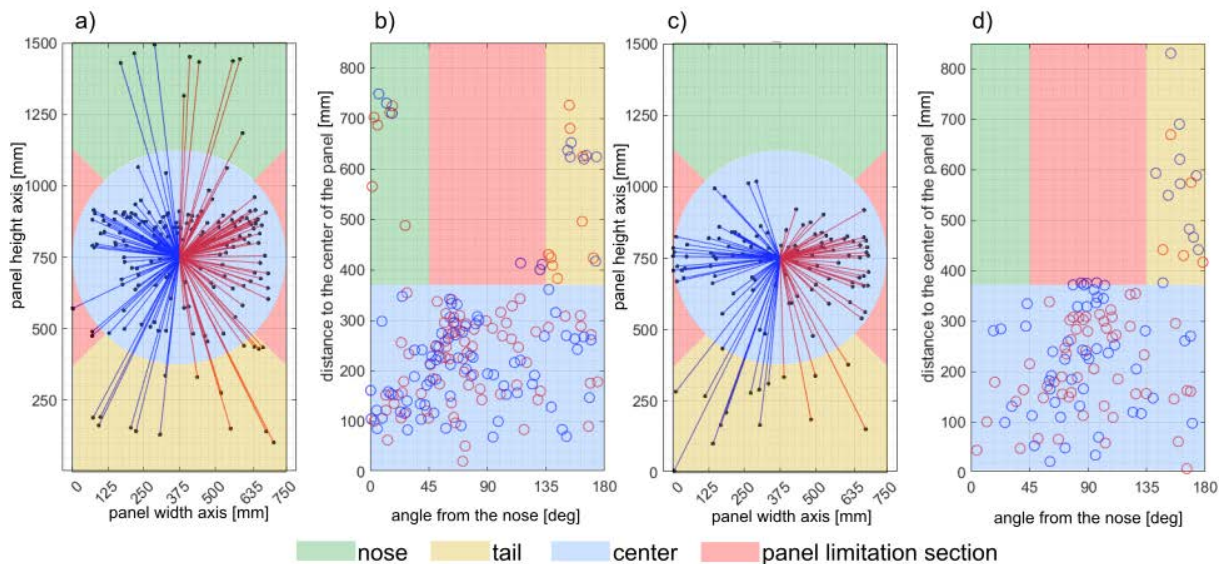


Figure 6. Liner case fragment density with section colour coding for detonation in air (a), (b) and charge top at surface (c), (d).

The background colour indicates one of the reference fragmentation areas. It is notable that no fragment hit the 'nose area' when the charge was fully submerged. For all three shell types, the light blue area represents the highest fragment density and a launch angle between 59° and 90°, which generates a close throw distance. The light red, called the 'limitation section', refers to the left and right side of the charge. This red section in Figure 6 (b) and (d) represents the area in which few metal pieces were recorded due to the panel width of 750 mm, but more possible fragment traces are expected beyond the strawboard edge.

In all tests, the fragment distribution is symmetrical about the longitudinal axis of symmetry of the panel and the main fragment concentration is in the middle area of the strawboard. Additionally, a higher number of hits was observed in the tail section compared to the nose when water was present.

The results of HSV recordings and postprocessing

The tests were recorded at a frame rate of 100,000-150,000 frames per second (fps) enabling the capture of the flight path of fragments. Figure 7 shows frames representing each of the three different fragmentation shells at different depths. A balance of shutter speed and additional lighting is the key to quality records in low or very dark conditions. In plot (a) the charge detonates in the air, the main source of intense light is the explosive material itself. A faster shutter speed enabled visualisation of the fragments ahead of the bright flash of the explosion. In Figure 7 (b) and (c), the charge is submerged beneath the water surface and therefore the illumination of the scene comes from the ambient lighting conditions.

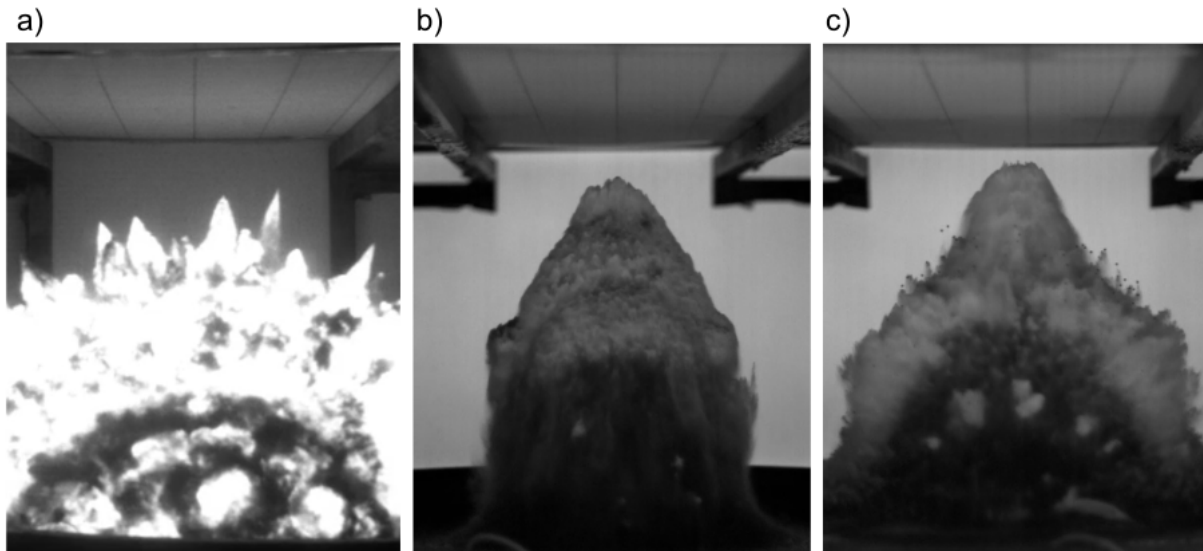


Figure 7. High speed video (HSV) recording showing a range casing and depth combinations, for illustrative purposes a) 1.7 mm balls in air (A), b) machined liner at 45 mm (D), c) 2.6 mm balls at 95 mm (E).

Although flight characteristics of all three fragment types were obtained, it is not possible to assign the mass of the irregular steel liner fragments to the recorded trajectory. Not only due to the registration of a two-dimensional image, but also the possible division of the fragments into smaller elements upon impact with the witness panel. This means that velocities can be established, but momentum can only be found for the two bearing cases where the fragments were of a known mass.

In order to establish the velocity of the fragments from the HSV recordings, a Matlab script was used to track the breakout from the centre of the charge. This assumed a 2-D plane of fragments around the circumference of the charge, and as such could potentially underestimate the travel distance and thus the fragment velocity. As seen in Figure 4, this is a reasonable assumption for a large proportion of the fragments, which can be seen in a narrow band on the strawboard.

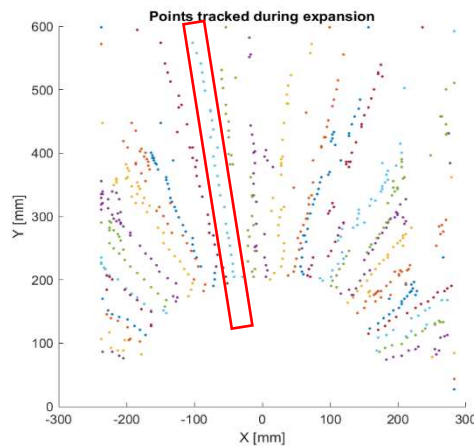
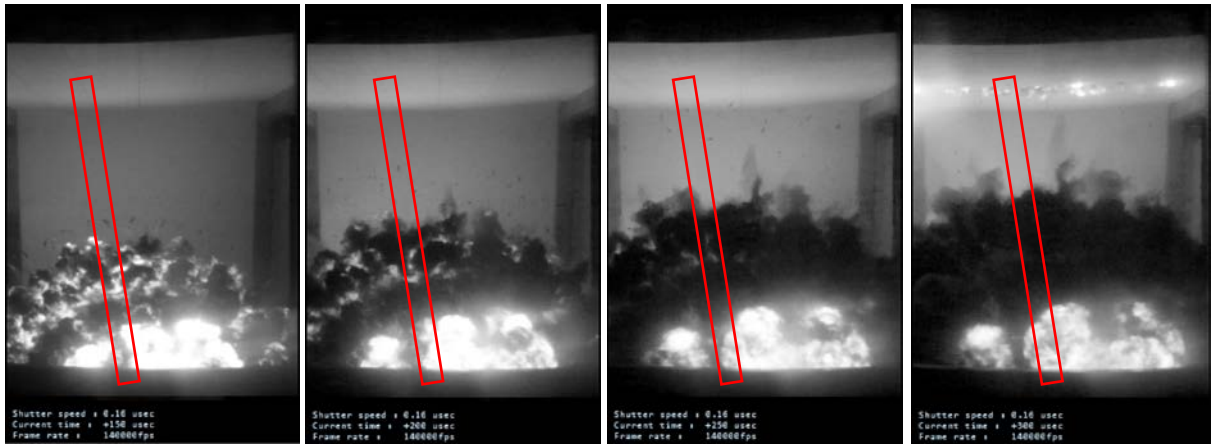


Figure 8. Results showing fragment flight trajectory, obtained using high-speed video processing of the machined liner detonation in air

First, a calibration image was used (with a physical distance marker in view of the camera) to establish the size of a given pixel. After this, image subtraction was employed to identify differences between subsequent frames, filtered by an intensity threshold to reduce the effect of sensor noise – as previously utilised by Farrimond et al. [18]. The 180° zone above the charge was discretised into 5° sectors and the furthest point of difference in each sector was identified as the ejecta front. HSV frames from one test and the associated tracking data are shown in Figure 8, with a tracked fragment highlighted in red. Once the fragments were successfully tracked, the displacement from the charge centre could be plotted against time to establish fragment velocity.

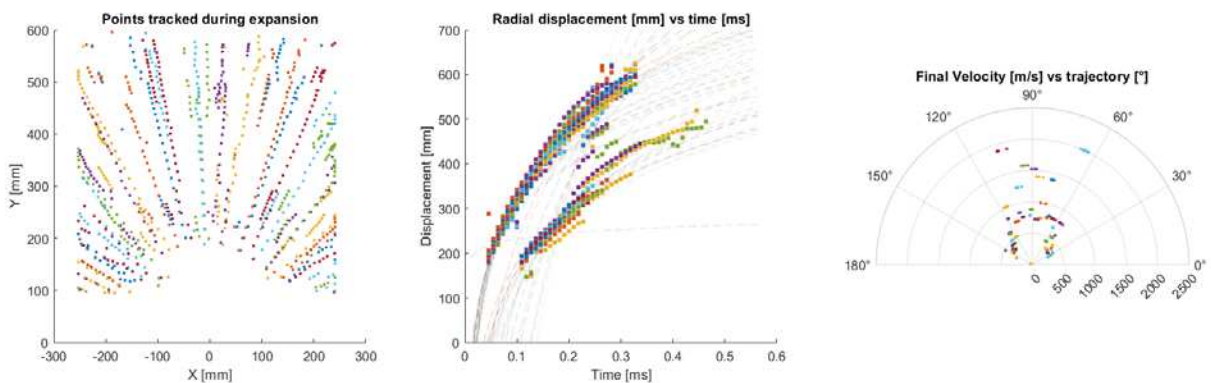


Figure 9. Fragment tracking of 1.7mm bearing tests with water to charge centre. (Series 4).

A log fit was used to characterise the initial fast high velocity of the fragments as they were accelerated by the charge, followed by the deceleration due to air and water resistance effects. This is shown in Figure 9, wherein it can be seen that a higher fragment velocity was evaluated above the

charge than for those with horizontal travel vectors. 'Final velocity' is determined as the fragment velocity at 550 mm away from the charge centre (i.e. just before striking the strawboard), and thus will in future allow for comparison against the velocities inferred from the strawboard measurements.

Conclusion / Summary / Recommendations

Experimental explosive tests and numerical simulations are the basis for common regulations, simple calculations, and tables for blast and fragmentation hazard prediction for an air detonation. Explosive Ordnance Disposal technicians can use this information during munition or IED disposal to assess the hazard and mitigate the risk of human injury and property damage. For naval munitions located below the water surface, the risk of fragmentation cannot be ignored, but there is no common method in military procedures for calculating safe distance as a function of depth.

Despite limitations related to charge mass and case design, the presented results show a clear relationship between detonation depth and the fragmentation behaviour of the steel shell.

To ensure proper protection against fragments in the maritime domain, ordnance disposal procedure needs to account for this.

Based on small explosive tests the fragment parameters and the damping properties of water were demonstrated by direct comparisons between explosions in air and within varying depths of water. Further studies will compare this small-scale work against the full-scale testing conducted previously, available within the literature [11], in order to ascertain the validity of small-scale trials for underwater explosion and fragmentation analyses.

Acknowledgements

This work has been supported by the Polish National Agency for Academic Exchange (NAWA) under the STER programme, Towards Internationalization of Poznan University of Technology Doctoral School (2022-2024). A portion of the experimental work was funded by the Defence Science and Technology Laboratory (Dstl). Additionally, the assistance of the technical staff at the University of Sheffield and support of Blastech Ltd in preparing the facility and conducting the experimental work is gratefully acknowledged.

References

- [1]. Hand grenades - Designed for operational effectiveness, Australian Munitions, 2016.
- [2]. Army TM 5-1300, Structures to Resist the Effects of Accidental Explosions, Départements of the Army, the Navy and the Air Force, 1990
- [3]. United Nations Office for Disarmament Affairs (UNODA), International Ammunition Technical Guidelines 01.80, Formulae for ammunition management, 2021.
- [4]. Absil, L.H.J, Kodde, H.H, and Weerheijm, J. Evaluation of Safety Distances for UXO Disposal Operations, TNO Prins Maurits Laboratory, Research Group Explosion Prevention and Protection, 1996.
- [5]. Zaker, T.A., Fragment and Debris Hazards, Department of Defense Explosives Safety Board Technical paper 12,1975.
- [6]. Zecevic, B., Catovic, A., and Terzic, J., Comparison of Lethal Zone Characteristics of Several Natural Fragmenting Warheads, Central European Journal of Energetic Materials, 2008, 5(2), 67-81. ISSN 1733-7178.
- [7]. Qi, R., Langdon G.S., Cloete, T.J., Chung Kim Yuen S., Behaviour of a blast-driven bearing embedded in rear detonated cylindrical explosive, International Journal of Impact Engineering 146, 2020.

- [8]. Zhao, Ch., Wang, S., Guo, C., Liu, D., Ma, F., Experimental study on fragmentation of explosive loaded steel projectile, *International Journal of Impact Engineering*, Volume 144, 2020, 103610, ISSN 0734-743X, <https://doi.org/10.1016/j.ijimpeng.2020.103610>.
- [9]. Schunck, T.; Eckenfels, D. Experimental Study of Explosion Mitigation by Deployed Metal Combined with Water Curtain. *Appl. Sci.* 2021, 11, 6539. <https://doi.org/10.3390/app11146539>
- [10]. Salter, S.H., Parkes, J.H., *The Use of Water-filled Bags to Reduce the Effects of Explosives*, The University of Edinburgh, 1994
- [11]. Swisdak, M.M. and Montanaro. P.E., *Hazards from Underwater Explosions - Naval Surface Warfare Center*, 1992.
- [12]. Lee, J. J. and Rude, G., *Underwater fragmentation of cylinders*. Defence R&D Canada. 2006.
- [13]. Farrimond, D., Ratcliff, A., Dennis, A., Rigby, S.E., Tyas, A., Clarke, S.D., Lodge, T.L., Tolman, W. MicroBlast - a benchmarking study of gramme-scale explosive trials. In: *Proceedings of the 26th International Symposium on Military Aspects of Blast and Shock (MABS26)*, Australia, 2023.
- [14]. "Assessing explosives safety risks, deviations, and consequences", Technical Paper 23, Department of Defense Explosives Safety Board and Service Representatives, 2019.
- [15]. Stanag 2884 - Underwater munition disposal procedures – General instructions, procedures and techniques - AEODP-01, 2014.
- [16]. *A guide to survey and clearance of Underwater Explosive Ordnance*, GICHD, 2015.
- [17]. Nowak, P., Neutralizacja historycznego uzbrojenia wojskowego o dużym wagoniarze materiału wybuchowego w ramach oczyszczania akwenów z przedmiotów wybuchowych i niebezpiecznych, *Rocznik Bezpieczeństwa Morskiego*, ISSN: 1898-3189, 2021.
- [18]. Farrimond DG, Rigby SE, Clarke SD, Tyas A. Time of arrival as a diagnostic for far-field high explosive blast waves. *International Journal of Protective Structures*. 2022;13(2):379-402. doi:10.1177/20414196211062923